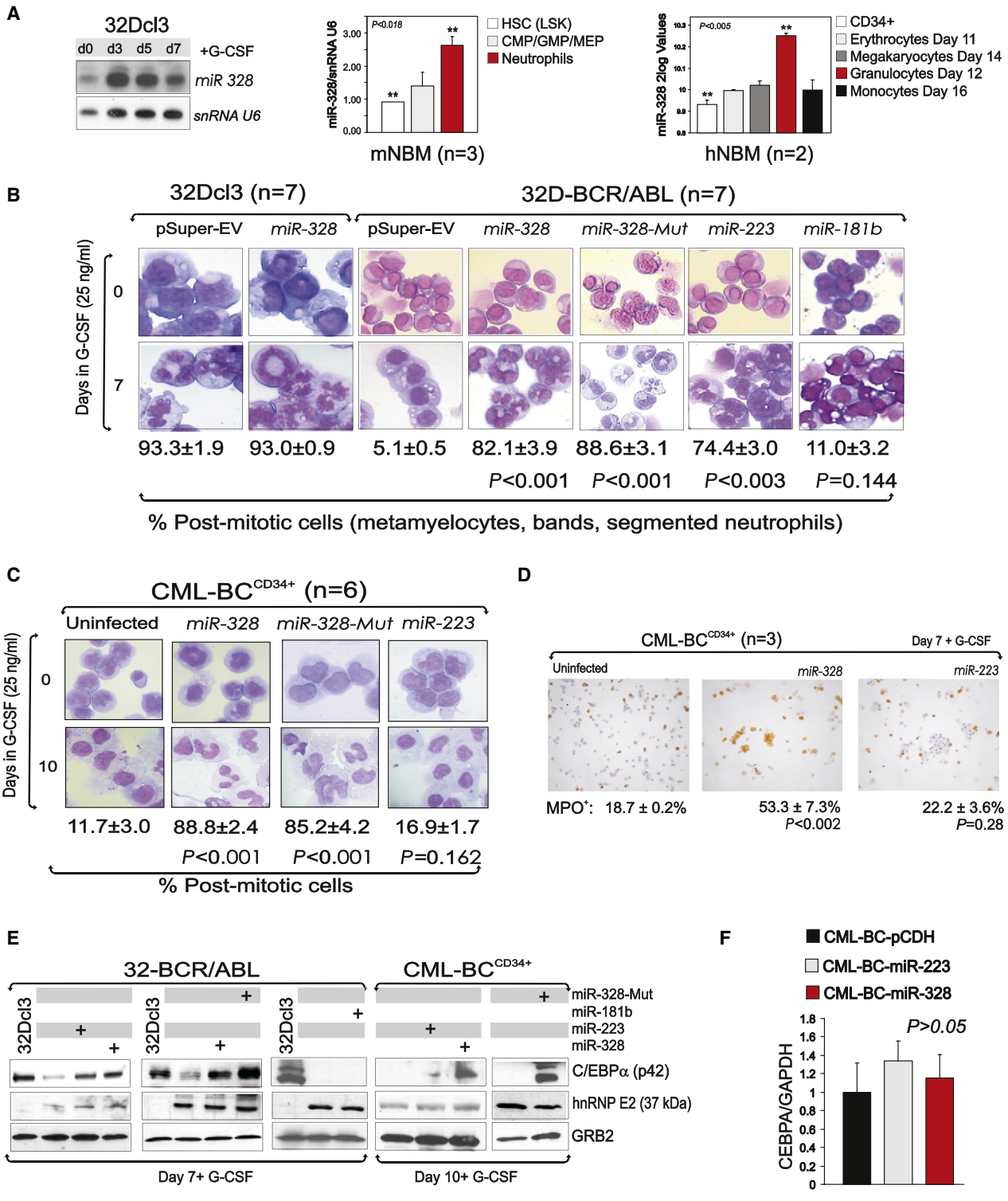

Figure 4. miR-328 Rescues Granulocytic Differentiation through Restoration of C/EBPα Expression

(A) miR-328 levels in (left) 32Dcl3 cells undergoing G-CSF-induced differentiation; (middle) $Lin^-/Sca^+/Kit^+$ HSC, CMP/GMP/MEP committed progenitors and mature neutrophil BM subpopulations from wild-type C57BL/6 mice (mean ± SEM); and (right) $CD34^+$ human BM cells undifferentiated (white) and induced to differentiate for the indicated time toward the erythroid (light gray), megakaryocytic (dark gray), granulocytic (red), or monocytic (black) lineages (mean ± SEM). (B) Wright-Giemsa-stained cytospins of G-CSF-treated (0–7 days) pSuper-, miR-328-, miR-328-Mut-, miR-223-, and/or miR-181b-infected 32Dcl3 and/or 32D-BCR/ABL cells (mean ± SEM). Levels of miR-223 in BCR/ABL^+ cell lines and primary cells and effect of ectopic miR-223 on cell proliferation are reported in Figure S2.

and G-CSF-driven differentiation in miR-328-transduced GFP$^+$ BCR/ABL$^+$ cell lines, BCR/ABL$^+$ Lin$^-$ mouse BM, and/or CML-BC^{CD34+} cells. As controls, we assessed the effects of ectopic miR-328-Mut, miR-181b, and the myeloid differentiation-related (Chen et al., 2004) miR-223 in BCR/ABL$^+$ cells. Of note, ectopic miR-328 or miR-223 levels in BCR/ABL$^+$ cells were similar to those in nontransformed cells (Figure 2D and Figure S2A), thus excluding off-target effects due to overexpression.

Although endogenous miR-328 (Figure 1) and, to a lower extent, miR-223 (Figure S2B) were downregulated in 32D-BCR/ABL and K562 cells, their ectopic expression did not have a significant effect on IL-3-dependent and/or -independent growth (Figure S2B). Likewise, ectopic miR-328 did not accelerate the kinetics of 32Dcl3 neutrophil maturation (Figure 4B), consistent with the barely detectable levels of hnRNP E2 in 32Dcl3 cells (Perrotti et al., 2002) and the increased expression of endogenous miR-328 in 32Dcl3, human CD34$^+$ (n = 2) and mouse Lin$^-$/Sca$^+$/Kit$^+$ (n = 3) BM (NBM) progenitors undergoing granulocytic differentiation (Figure 4A). Conversely, miR-328 levels were not significantly different in normal CD34$^+$ BM cells before and after differentiation toward other hematopoietic lineages (Figure 4A). As expected (Fazi et al., 2005), miR-223 enhanced 32Dcl3 differentiation (not shown).

In agreement with the potential role of miR-328 as an antagonist of hnRNP E2 differentiation inhibitory activity, forced expression of miR-328 at physiological levels (Figure 2D and Figure S2A) efficiently rescued granulocytic differentiation of newly established (15 days after BCR/ABL infection) 32D-BCR/ABL cells (Figure 4B). In fact, the majority (82.1% ± 3.9%) of miR-328-expressing 32D-BCR/ABL cells were postmitotic metamyelocytes, bands, and segmented neutrophils after 7 days of G-CSF-supplemented culture (Figure 4B). As expected, G-CSF-treated vector- and miR-181b-transduced BCR/ABL$^+$ cells remained blasts (5.1% ± 0.5% and 11.0% ± 3.2% postmitotic cells) (Figure 4B). By contrast, miR-328-Mut expression efficiently induced 32D-BCR/ABL differentiation (88.6% ± 3.1% postmitotic cells) (Figure 4B).

Although terminal differentiation was also a characteristic of miR-223-overexpressing 32D-BCR/ABL cells, only ectopic miR-328 but not miR-223 expression (Figure S2C) restored G-CSF-driven maturation of GFP$^+$ CD34$^+$ BM progenitors from myeloid CML-BC patients (n = 6) (Figure 4C). In fact, both miR-328- and miR-328-Mut-expressing CML-BC^{CD34+} BM cultures became bands and segmented neutrophils (88.8% ± 2.4% and 85.2% ± 4.2% postmitotic cells) after 10 days in rhG-CSF (25 ng/ml). By contrast, morphology of miR-223-expressing CML-BC^{CD34+} (n = 6) progenitors remained similar to untransduced cells (n = 6), appearing arrested at the myeloblast stage after 7–10 days in G-CSF-containing medium (16.9% ± 1.7% postmitotic cells) (Figure 4C) with unchanged levels of the granulocyte/macrophage markers CD11b or CD14 (not shown).

Consistent with the essential role of C/EBPα in neutrophil maturation of BCR/ABL$^+$ blasts (Ferrari-Amorotti et al., 2006; Perrotti et al., 2002; Wagner et al., 2006), C/EBPα expression was readily detectable in miR-223- and miR-328-transduced 32D-BCR/ABL myeloid precursors, and in miR-328- but not miR-223-expressing CML-BC^{CD34+} BM progenitors and miR-181b-expressing 32D-BCR/ABL cells (Figure 4E). This was dependent neither on hnRNP E2 downregulation (Figure 4E) nor on increased *CEBPA* mRNA levels (Figure 4F and Figure S2C). In agreement with its ability to bind hnRNP E2, miR-328-Mut also restored C/EBPα expression (Figure 4E), indicating that the differentiation-promoting effects of miR-328 do not result from the seed sequence-dependent silencing of miR-328 mRNA targets. Furthermore, myeloperoxidase (MPO), a marker of granulocyte/macrophage commitment and a direct transcriptional target of C/EBPα (Rosmarin et al., 1989; Wang et al., 2001), was also significantly increased in G-CSF-cultured miR-328- (18.7% ± 0.2% [uninfected] versus 53.3% ± 7.3% [miR-328]; $p < 0.004$) but not miR-223- (18.7% ± 0.2% [uninfected] versus 22.2% ± 3.6% [miR-223]; $p = 0.28$) expressing CML-BC^{CD34+} cells (n = 3) (Figure 4D). Finally, the dissimilar response of miR-223-transduced 32D-BCR/ABL versus CML-BC^{CD34+} progenitors to G-CSF might depend on differences in the mechanism(s) controlling expression of NFI-A (Figure S2D), a miR-223-negative regulator (Fazi et al., 2005).

miR-328 Restores *CEBPA* mRNA Translation Both In Vitro and In Vivo

As hnRNP E2:miR-328 binding in vitro is more efficient than that of *CEBPA* uORF (Figure 2), and miR-328 expression antagonizes hnRNP E2:*CEBPA* interaction (Figures 2D and 2E) most likely by competing for binding to hnRNP E2, it is plausible that miR-328 releases *CEBPA* from the translation inhibitory effects of hnRNP E2. Thus, we assessed the effect of miR-328 on *CEBPA* translation in rabbit reticulocyte lysate and in an in vivo mouse model of myeloid CML-BC. In the latter, BCR/ABL$^+$ cell differentiation is driven solely by ectopic C/EBPα expression, which is under the control of its uORF/spacer mRNA element (Chang et al., 2007). As reported (Perrotti et al., 2002), translation of *CEBPA* mRNA was markedly impaired (~80% inhibition) in in vitro translation reactions programmed with a *CEBPA* construct containing the uORF/spacer intercistronic region (pcDNA3-WT-uORF-C/EBPα) and the recombinant fusion protein MBP-hnRNP E2 (Figure 5A) but not when performed in the absence of exogenous hnRNP E2 (Figure 5A). Addition of 1000-fold excess of mature miR-328 but not miR-330 resulted in an almost 100% increase of newly synthesized ^{35}S-C/EBPα protein (*CEBPA*+hnRNP E2

(C) Wright-Giemsa-stained cytospins of primary G-CSF-treated (0–10 days) uninfected and miR-328-, miR-328-Mut-, and miR-223-infected CML-BC^{CD34+} BM progenitors (mean ± SEM). For levels of ectopic miR-328 and miR-223 expression in primary CML-BC cells, see Figure S2.

(D) Myeloperoxidase (MPO) immunostaining of G-CSF-treated uninfected and miR-328- and miR-223-transduced CML-BC^{CD34+} BM cells. Data are representative of three independent experiments (mean ± SEM).

(E) Western blot shows C/EBPα, hnRNP E2, and GRB2 levels in G-CSF-treated 32Dcl3 and empty vector-, miR-328-, miR-223-, miR-328-Mut-, and/or miR-181b-infected 32D-BCR/ABL and CML-BC^{CD34+} BM cells (right).

(F) qRT- PCR shows levels of *CEBPA* in empty vector-, miR-223-, or miR-328-infected CML-BC cells (mean ± SEM). qRT- PCR showing *CEBPA* mRNA levels in empty vector-, miR-223-, or miR-328-transduced 32D-BCR/ABL cells (mean ± SEM) is reported in Figure S2.

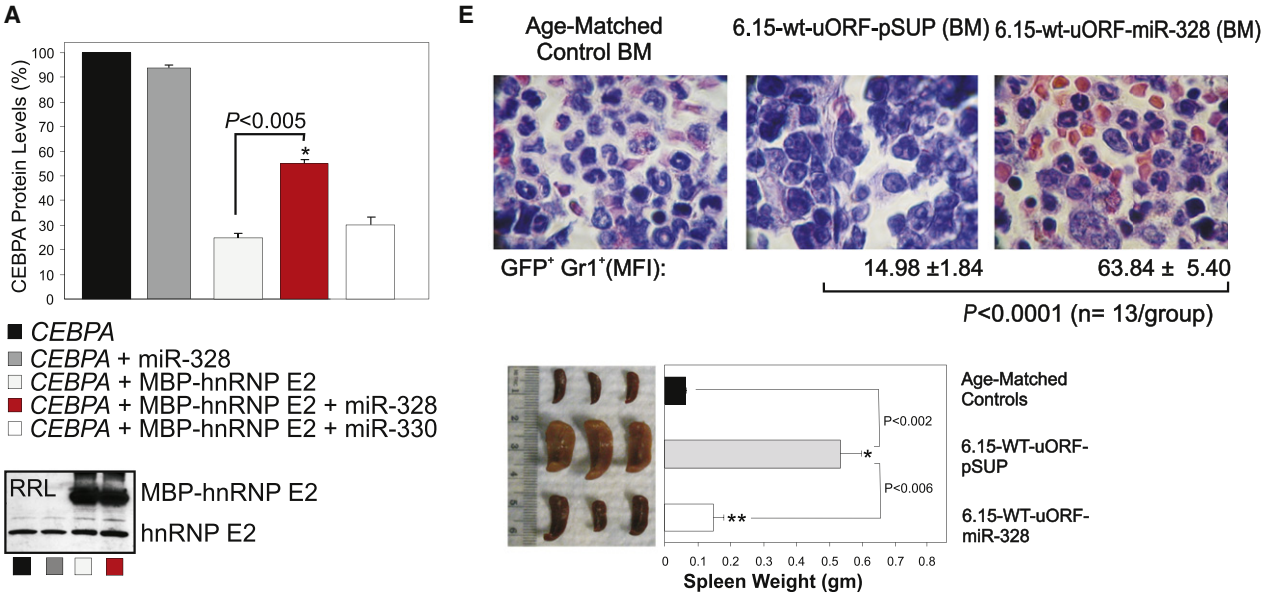
A
CEBPA Protein Levels (%)
P<0.005
CEBPA
CEBPA + miR-328
CEBPA + MBP-hnRNP E2
CEBPA + MBP-hnRNP E2 + miR-328
CEBPA + MBP-hnRNP E2 + miR-330
RRL
MBP-hnRNP E2
hnRNP E2
E
Age-Matched Control BM
6.15-wt-uORF-pSUP (BM)
6.15-wt-uORF-miR-328 (BM)
GFP+ Gr1+(MFI):
14.98 ±1.84
63.84 ± 5.40
P<0.0001 (n= 13/group)
P<0.002
P<0.006
Age-Matched Controls
6.15-WT-uORF-pSUP
6.15-WT-uORF-miR-328
Spleen Weight (gm)

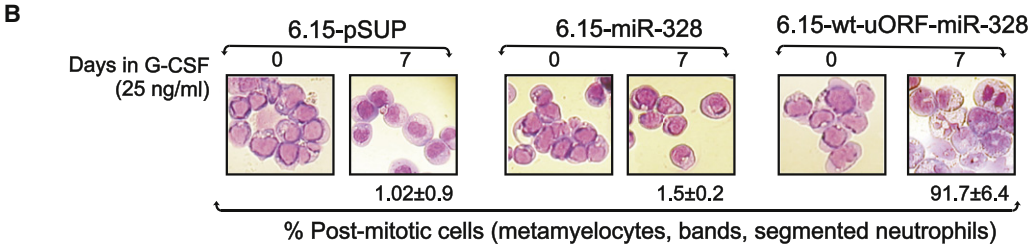
B
Days in G-CSF (25 ng/ml)
6.15-pSUP
6.15-miR-328
6.15-wt-uORF-miR-328
0
7
1.02±0.9
1.5±0.2
91.7±6.4
% Post-mitotic cells (metamyelocytes, bands, segmented neutrophils)

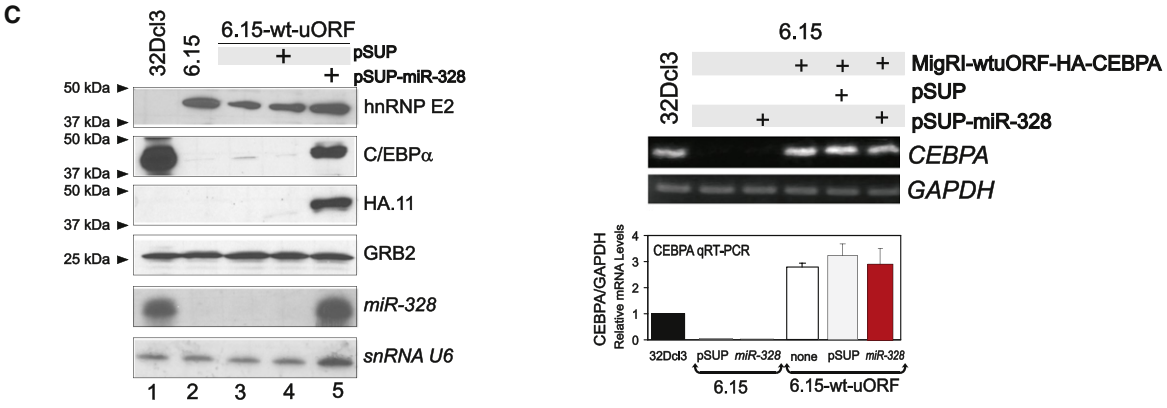
C
32Dcl3
6.15
6.15-wt-uORF
pSUP
pSUP-miR-328
50 kDa
37 kDa
25 kDa
hnRNP E2
C/EBPα
HA.11
GRB2
miR-328
snRNA U6
1 2 3 4 5
MigRI-wtuORF-HA-CEBPA
CEBPA
GAPDH
CEBPA qRT-PCR
CEBPA/GAPDH Relative mRNA Levels
32Dcl3 pSUP miR-328 none pSUP miR-328
6.15
6.15-wt-uORF

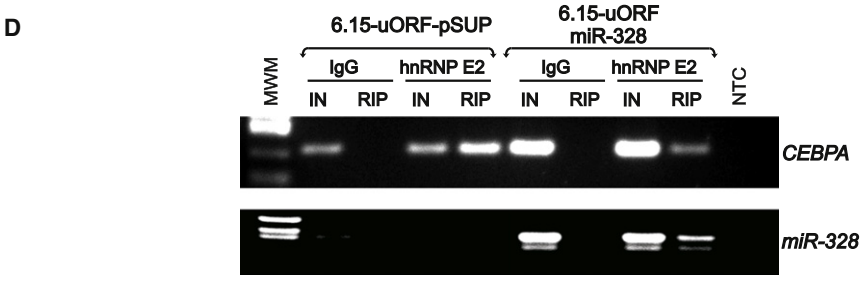
D
6.15-uORF-pSUP
6.15-uORF miR-328
MWM
IgG
hnRNP E2
IN
RIP
NTC
CEBPA
miR-328

versus *CEBPA*+hnRNP E2+miR-328; $p < 0.005$) (Figure 5A). Note that addition of miR-328 in the absence of MBP-hnRNP E2 did not significantly affect *CEBPA* mRNA translation (Figure 5A). Moreover, the large amount of MBP-hnRNP E2 (Figure 5A) might justify the incomplete rescue of *CEBPA* translation.

To assess whether forced miR-328 expression rescues neutrophilic maturation of differentiation-arrested BCR/ABL$^+$ blasts through restoration of *CEBPA* mRNA translation, we used the aberrant 32D-BCR/ABL long-term cultured 6.15 cell clone that exhibits extremely high levels of BCR/ABL and hnRNP E2 but is unable to undergo G-CSF-driven differentiation due to transcriptional suppression of CEBPα expression (Figure 5C). Indeed, 6.15 cells completely rely on translation of ectopic *CEBPA* mRNA for differentiation. Thus, parental and 6.15 cells expressing a GFP-WT-uORF/spacer-C/EBPα (6.15-WT-uORF), which contains the hnRNP E2 translation inhibitory element, were retrovirally transduced with the pSUPERIOR-retro-puro-miR-328 (6.15-WT-uORF-miR-328) or with the empty vector (6.15-WT-uORF-pSUP). Differentiation assays confirmed that the ability of miR-328 to induce neutrophil maturation is dependent on and mediated by the presence of *CEBPA* mRNA, as expression of miR-328 in parental 6.15 cells failed to rescue differentiation, whereas 91.7% ± 6.4% of 6.15-WT-uORF-miR-328 cells were postmitotic after 7 days of culture in G-CSF (Figure 5B). Furthermore, forced miR-328 expression neither decreased hnRNP E2 protein nor increased *CEBPA* mRNA levels (Figure 5C), suggesting that the restoration of C/EBPα protein expression in 6.15-WT-uORF-miR-328 cells (Figure 5C) results from the ability of miR-328 to interfere with hnRNP E2 translation inhibitory activity. Accordingly, anti-hnRNP E2 RIP assays performed with 6.15-WT-uORF-pSUP and 6.15-WT-uORF-miR-328 lysates revealed that miR-328 expression and, therefore, formation of the hnRNP E2:miR-328 complex (Figure 5D) markedly decreased levels of the hnRNP E2-bound *CEBPA* mRNA (Figure 5D).

To determine whether miR-328 influences the CML-BC-like disease process induced by transplantation of BCR/ABL-expressing cells, SCID mice (n = 13 per group) were intravenously injected with 6.15-WT-uORF-miR-328 or 6.15-WT-uORF-pSUP cells (5×10^5 GFP$^+$-puromycin-selected cells/mouse), and engraftment was assessed 1 week later by nested RT-PCR-mediated BCR/ABL detection in peripheral blood (not shown). After 3 weeks, three mice/group were sacrificed for visual and histopathologic examination of hematopoietic organs and for flow cytometric quantification of GFP$^+$/GR1$^+$ differentiated BM cells. Consistent with the almost complete hnRNP E2-dependent translational inhibition of C/EBPα expression in 6.15-WT-uORF cells (Chang et al., 2007), hematoxylin/eosin-stained sections of BM (Figure 5E), spleen, and liver (not shown) from 6.15-WT-uORF-pSUP-injected mice showed splenomegaly and massive infiltration of myeloid blasts with a low degree of differentiation. A few myeloid cells undergoing terminal neutrophil differentiation were occasionally observed in BM from 6.15-WT-uORF-pSUP-injected mice (mean fluorescence intensity [MFI]: 14.98 ± 1.84 GFP$^+$/GR1$^+$ BCR/ABL$^+$ cells). By contrast, spleens from 6.15-WT-uORF-miR-328-injected mice appeared normal in weight or slightly hyperplastic, and histopathologic analysis of BM (Figure 5E), spleen, and liver (not shown) showed marked infiltration by mature neutrophils and myeloid precursors at postmitotic stages of differentiation (MFI: 63.84 ± 5.40 GFP$^+$/GR1$^+$ BCR/ABL$^+$ cells) when compared to age-matched controls (Figure 5E), suggesting that miR-328 also negatively regulates survival pathways in CML-BC although its major effect appears to be on differentiation. In fact, although no significant difference in survival time was noted, the remaining 6.15-WT-uORF-pSUP-injected mice died of a CML-BC-like leukemia, whereas 6.15-WT-uORF-miR-328-injected animals succumbed from an aggressive CML-CP-like myeloproliferative disorder (not shown). Altogether, these in vitro and in vivo results indicate that rescue of granulocytic maturation of differentiation-arrested BCR/ABL$^+$ cells by miR-328 is likely due to its direct binding to hnRNP E2 that, in turn, prevents translational inhibition of *CEBPA* mRNA.

A BCR/ABL-MAPK-hnRNP E2 Pathway Suppresses miR-328 Transcription through Inhibition of C/EBPα

We recently reported that high levels of BCR/ABL expression/kinase activity, as observed in CML-BC (Jamieson et al., 2004; Schultheis et al., 2005), impair C/EBPα expression through the MAPK(ERK1/2)-dependent regulation of hnRNP E2 expression/activity (Chang et al., 2007). To determine whether BCR/ABL uses the same signaling pathway to suppress miR-328 expression in CML-BC, miR-328 levels were evaluated in G-CSF-cultured (24–48 hr) parental and newly established 32D-BCR/ABL cells treated with imatinib (2 μM) or MEK1 inhibitors U0126 (25 μM) and CI-1040 (10 μM) and after overexpression (MSCV-Flag-E2)

Figure 5. In Vitro and In Vivo Interference of miR-328 with hnRNP E2 Translation Inhibition of C/EBPα Expression

(A) Levels of newly synthesized ^{35}S-C/EBPα protein in RRL translation reactions programmed with *CEBPA* mRNA (derived from pcDNA3-WT-uORF-C/EBPα) (black), *CEBPA* mRNA and mature miR-328 RNA oligonucleotides (dark gray), *CEBPA* mRNA and recombinant MBP-hnRNP E2 protein either alone (light gray) or in the presence of mature miR-328 (red), or miR-330 (white; negative control) RNA oligonucleotides. Data are expressed as percentage of the mean ± SEM and are representative of three different experiments performed in duplicate. Inset: Western blot shows levels of both endogenous RRL hnRNP E2 and recombinant MBP-hnRNP E2.

(B) Wright-Giemsa-stained cytospins of G-CSF-treated (0–7 days) 6.15-pSUP, 6.15-miR-328, and 6.15-WT-uORF-miR-328 cells (mean ± SEM).

(C) Left: Levels of hnRNP E2, endogenous and HA-tagged C/EBPα, and GRB2 proteins and miR-328 and snRNA U6 in parental 32Dcl3, 6.15-pSUP-transduced, and miR-328-transduced 6.15-WT-uORF cells; right: RT-PCR and qRT-PCR show levels of *CEBPA* mRNA in 32Dcl3, 6.15, 6.15-miR-328, and 6.15-WT-uORF-HA-CEBPA cells either uninfected or infected with pSUP or miR-328 constructs. *GAPDH* levels were measured for normalization (mean ± SEM).

(D) RIP assays for *CEBPA* mRNA (top) and miR-328 (bottom) on anti-hnRNP E2 (lanes 5 and 9) and nonrelated IgG (lanes 3 and 7) IPs from 6.15-uORF-pSUP (lanes 2–5) and 6.15-uORF-miR-328 cells (lanes 6–9). IN: input RNA.

(E) Top: H&E-staining of BM shows maturation of BCR/ABL$^+$ cells in mice injected with p-SUPERIOR vector- (middle) and miR-328-transduced (right) 6.15-WT-uORF cells. Age-matched mice (left) served as a control. FACS analysis shows mean fluorescence intensity (MFI; mean ± SEM) of differentiated GFP$^+$Gr1$^+$BCR/ABL$^+$ cells at 3 weeks post-transplant from BM of 3 mice/group. Bottom: Visual analysis and weight of spleens from the same groups of mice (mean ± SEM).

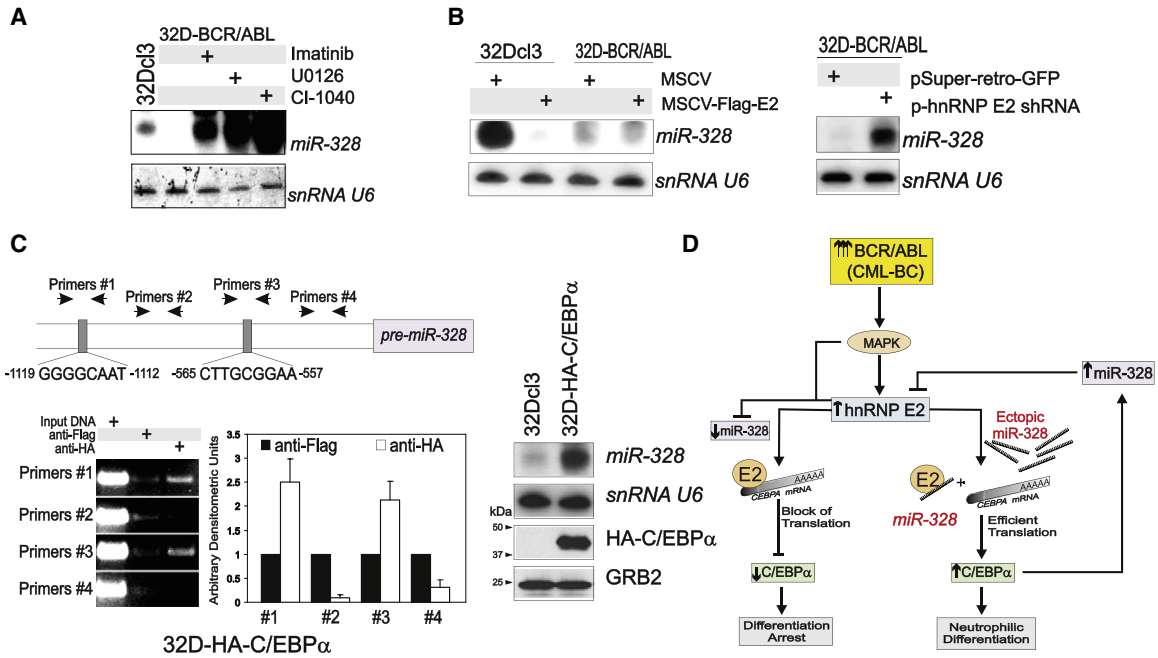

Figure 6. Pathways Regulating miR-328 Expression

miR-328 levels in 32Dcl3 and/or 32D-BCR/ABL cells (A) treated with imatinib or the MAPK inhibitors U0126 and CI-1040 or (B) expressing a Flag-hnRNP E2 (left) or a shRNA-targeting hnRNP E2 (right).

(C) Top: Representation of the C/EBPα-binding sites within the miR-328 promoter; bottom: Chromatin immunoprecipitation (ChIP) with anti-HA antibody shows binding of HA-C/EBPα to miR-328 promoter sequences in 32D-HA-C/EBPα cells (left: ChIP blot; middle: densitometric analysis). Anti-Flag immunoprecipitates served as negative controls. Bars indicate the mean ± SEM from three independent experiments; northern and western blots (right) show levels of miR-328 and HA-C/EBPα, respectively, in parental and 32D-HA-C/EBPα cells. U6 snRNA and GRB2 protein levels were used as controls.

(D) Model of the molecular network regulating miR-328 expression in CML-BC and miR-328 *decoy activity* in BCR/ABL$^+$ myeloid cell differentiation by direct interference with hnRNP E2 translation inhibition of C/EBPα expression.

or shRNA-mediated downregulation (pSR-hnRNP E2 shRNA) of hnRNP E2. Inhibition of BCR/ABL or MEK1 kinases strongly enhanced miR-328 expression (Figure 6A), suggesting that BCR/ABL-mediated suppression of miR-328 requires MAPK(ERK) activity. Ectopic hnRNP E2 impaired miR-328 expression in 32Dcl3 cells, with no noticeable effect in 32D-BCR/ABL cells (Figure 6B) that already express high levels of hnRNP E2 (Perrotti et al., 2002). By contrast, shRNA-mediated downregulation of hnRNP E2 efficiently rescued miR-328 expression (Figure 6B). Thus, the BCR/ABL-MAPK-induced hnRNP E2 may directly regulate miR-328 nuclear export, processing, and/or stability or indirectly influence miR-328 transcription. Of interest, modulation of hnRNP E2 levels did not alter miR-223 expression in 32D-BCR/ABL cells, whereas hnRNP E2 overexpression inhibited miR-223 in 32Dcl3 cells (Figure S2E), consistent with the notion that hnRNP E2 reduces C/EBPα expression (Perrotti et al., 2002), thereby averting C/EBPα-dependent miR-223 transactivation (Fazi et al., 2005).

Transcription Element Search System-mediated (http://www.cbil.upenn.edu/cgi-bin/tess) sequence analysis revealed four putative C/EBPα-binding sites scattered within 1500 bp upstream of the mouse *pre-miR-328* (Figure 6C). Thus, chromatin immunoprecipitation (ChIP) assays were performed using nuclear extracts from GFP-sorted HA-C/EBPα-expressing 32Dcl3 cells (32D-HA-C/EBPα) and four sets of primers, each encompassing one of the potential C/EBPα-binding sites. In vivo physical interaction between HA-C/EBPα and the miR-328 promoter region was detected in ChIP assays performed on anti-HA but not anti-Flag (negative control) immunoprecipitates with primer sets #1 and #3 containing the human/mouse-conserved C/EBPα-binding sites located at nucleotides −1119 to −1112 and −565 to −557, respectively (Figure 6C). Accordingly, ectopic C/EBPα expression markedly induced miR-328 levels in myeloid precursors (Figure 6C), altogether suggesting that a BCR/ABL-MAPK-hnRNP E2 pathway downregulates miR-328 expression through inhibition of C/EBPα, thus impeding enhancement of miR-328 transcription (Figure 6D).

miR-328 Impairs CML-BC^{CD34+} Clonogenic Potential and Canonically Suppresses PIM1 Expression

Ectopic miR-328 expression reduced colony formation in 32D-BCR/ABL, Lin$^-$ SCLtTA-BCR/ABL (n = 5), and CML-BC^{CD34+} (n = 2) BM cells by 75%, 83%, and 75%, respectively (Figure 7A). The effect of miR-328 on clonogenicity of BCR/ABL$^+$ cells is independent from hnRNP E2:miR-328 interaction, as shRNA-mediated hnRNP E2 downregulation did not affect BCR/ABL-driven colony formation (Figure 7A). Thus, miRanda, PicTar, and TargetScan bioinformatics algorithms were utilized to identify miR-328 targets regulating CML-BC progenitor cell survival. Among the predicted miR-328 human/mouse mRNA targets,

PIM1 (Figure 7B) kinase is important for survival of BCR/ABL$^+$ cell lines (Nieborowska-Skorska et al., 2002). PIM1 protein was strongly upregulated in a BCR/ABL kinase-dependent manner in cell lines and CD34$^+$ CML-BC (n = 2) versus CML-CP and NBM BM cells (Figure 7C).

Ectopic miR-328 expression in 32D-BCR/ABL, K562, and CML-BC^{CD34+} cells decreased PIM1 protein without significantly affecting its mRNA levels (Figure 7D), suggesting that miR-328 might impair mRNA translation upon interaction with the *PIM1* 3′UTR. To formally demonstrate that miR-328 silences PIM1 expression through its interaction with the miR-328-binding site, we cloned the wild-type (pMX-Flag-WTPIM1-WT3′UTR) and miR-328-binding site-deleted (pMX-Flag-WTPIM1-Δ3′UTR) *PIM1* 3′UTR (Figure 7E) into a pMX-Flag-WTPIM1 plasmid and transduced these constructs into 32D-BCR/ABL-miR-328 or, as a negative control, 32D-BCR/ABL-miR-223 cells. As expected, ectopic Flag-PIM1 expression was lower in pMX-Flag-WTPIM1-WT3′UTR-transduced 32D-BCR/ABL-miR-328 cells but not in cells transduced with pMX-Flag-WTPIM1-Δ3′UTR or with *PIM1* cDNA only (pMX-Flag-WTPIM1) (Figure 7E). Accordingly, Flag-PIM1 expression derived from pMX-Flag-WTPIM1-WT3′UTR was barely detectable in miR-328- but not in miR-223-transduced cells, in which its expression was similar to that of Flag-WTPIM1 and Flag-WTPIM1-Δ3′UTR (Figure 7E), indicating that decreased ectopic PIM1 levels are not due to loss of other miRNA-binding sites within the 196 bp-deleted 3′UTR. Expression of the seed sequence-mutated mir-328 (miR-328-Mut) impaired the ability of miR-328 to canonically suppress PIM1 expression (Figure 7F). Thus, miR-328 specifically silences PIM1 expression through interaction with the *PIM1* 3′UTR. In agreement with the importance of PIM1 for survival of BCR/ABL$^+$ cells, expression of a wild-type *PIM1* cDNA lacking the 3′UTR (WT PIM1) but not of a kinase-deficient (KD PIM1) *PIM1* cDNA into 32D-BCR/ABL-miR-328 cells (Figure 7G) completely restored IL-3-independent colony formation (Figure 7G), suggesting that miR-328-dependent inhibition of BCR/ABL-driven clonogenic potential results from direct PIM1 downregulation. Note that WT PIM1 alone did not affect 32D-BCR/ABL-pSR-EV clonogenic potential (Figure 7G).

DISCUSSION

Altered miRNA expression has been tightly associated with cancer development and progression (Friedman et al., 2009; Garzon et al., 2006). Among the miRNAs differentially expressed in CML, we focused on miR-328 and provided a series of evidence highlighting two important concepts. The first represents a paradigm shift to the notion that miRNAs act primarily as negative posttranscriptional regulators of gene expression and proposes for miRNAs a function termed *decoy activity*. The second identifies miR-328 as a molecular relay, the loss of which is important for the differentiation arrest of progressing CML-BC blasts.

miR-328 Decoy Activity

As miRNAs base pair with mRNA 3′UTRs in a sequence-specific manner (Bartel, 2009), it is conceivable that miRNAs could interfere with the activity of RNA-binding proteins (e.g., hnRNPs), either indirectly by pairing with RBP-binding sites contained in specific mRNAs (George and Tenenbaum, 2006) or directly through binding the RBP itself and impeding RBP:mRNA interaction. Herein we demonstrated that miRNAs can act as direct inhibitors of RBP activity. In fact, miR-328 specifically interacts in a seed sequence-independent manner and, most likely, through its C-rich clusters, with the translational inhibitor poly (rC)-binding protein hnRNP E2. This, in turn, prevents and/or displaces *CEBPA* mRNA binding to hnRNP E2 and rescues *CEBPA* mRNA translation both in vitro and in vivo. In support of the notion that miR-328 and, most likely, other miRNAs may act as "decoy" molecules for RBPs, which upon binding could control synthesis, processing, export, stability, and/or translation of specific mRNA subsets, a proteomics-based study in epithelial A431 cells reported that forced miR-328 expression not only decreased levels of different genes but also upregulated a subset of proteins (Wang et al., 2008). Interestingly, 37% of these upregulated proteins have mRNAs with complex 5′UTRs (e.g., uORF or multiple ATGs) containing C-rich elements representing potential hnRNP E2-binding sites. Thus, it is reasonable to speculate that upregulation of some of these proteins might result from interference with hnRNP E2 activity. Furthermore, there is evidence that miRNAs, other components of the RISC complex (Parker and Sheth, 2007) and RBPs (e.g., hnRNP E2) are present in processing bodies (P bodies) (Fujimura et al., 2008), dynamic subcellular structures where mRNAs are complexed with RBPs and/or miRNAs for translational suppression or decay (Parker and Sheth, 2007). In this scenario, miR-328 may compete with *CEBPA* mRNA for binding to hnRNP E2 that, in turn, releases *CEBPA* and allows its loading onto polysomes for translation. It is also possible that hnRNP E2 not only prevents C/EBPα-dependent induction of pri-miR-328 transcription but also directly promotes miR-328 decay. Accordingly, an inverse correlation exists between hnRNP E2 and miR-328 expression in CML-BC, and hnRNP E2 more efficiently binds to miR-328 than to *CEBPA*. However, as hnRNP E2 continuously shuttles between nucleus and cytoplasm as well as in and out of P bodies (Fujimura et al., 2008; Makeyev and Liebhaber, 2002), knowledge of the subcellular location where initial binding of hnRNP E2 to miR-328 or *CEBPA* occurs remains elusive, although a plausible assumption is the cytoplasm as their association was detected using cytoplasmic extracts.

MicroRNA interaction with sequence-specific RBPs is not unprecedented; however, none of the reported mechanisms match the case of hnRNP E2 and miR-328. For example, hnRNP A1, another RBP upregulated in CML-BC (Perrotti and Neviani, 2007), binds the primary miR-17-92 transcript to allow processing of pre-miR-18a (Guil and Caceres, 2007). Interestingly, expression of the miR-17-92 cluster is upregulated in CML and is important for proliferation and reduced susceptibility to apoptosis of K562 cells (Venturini et al., 2007). However hnRNP E2:miR-328 interaction does not seem to affect miR-328 biogenesis, as no accumulation of primary or precursor miR-328 was detected in BCR/ABL$^+$ cells (not shown). It was also shown that miR-369-3 interacts with the AU-rich region (ARE) of *TNF-α* mRNA, which recruits the AGO2-FXR1 RBP complex to the ARE element itself and upregulates or represses translation under serum-starved or proliferating conditions, respectively

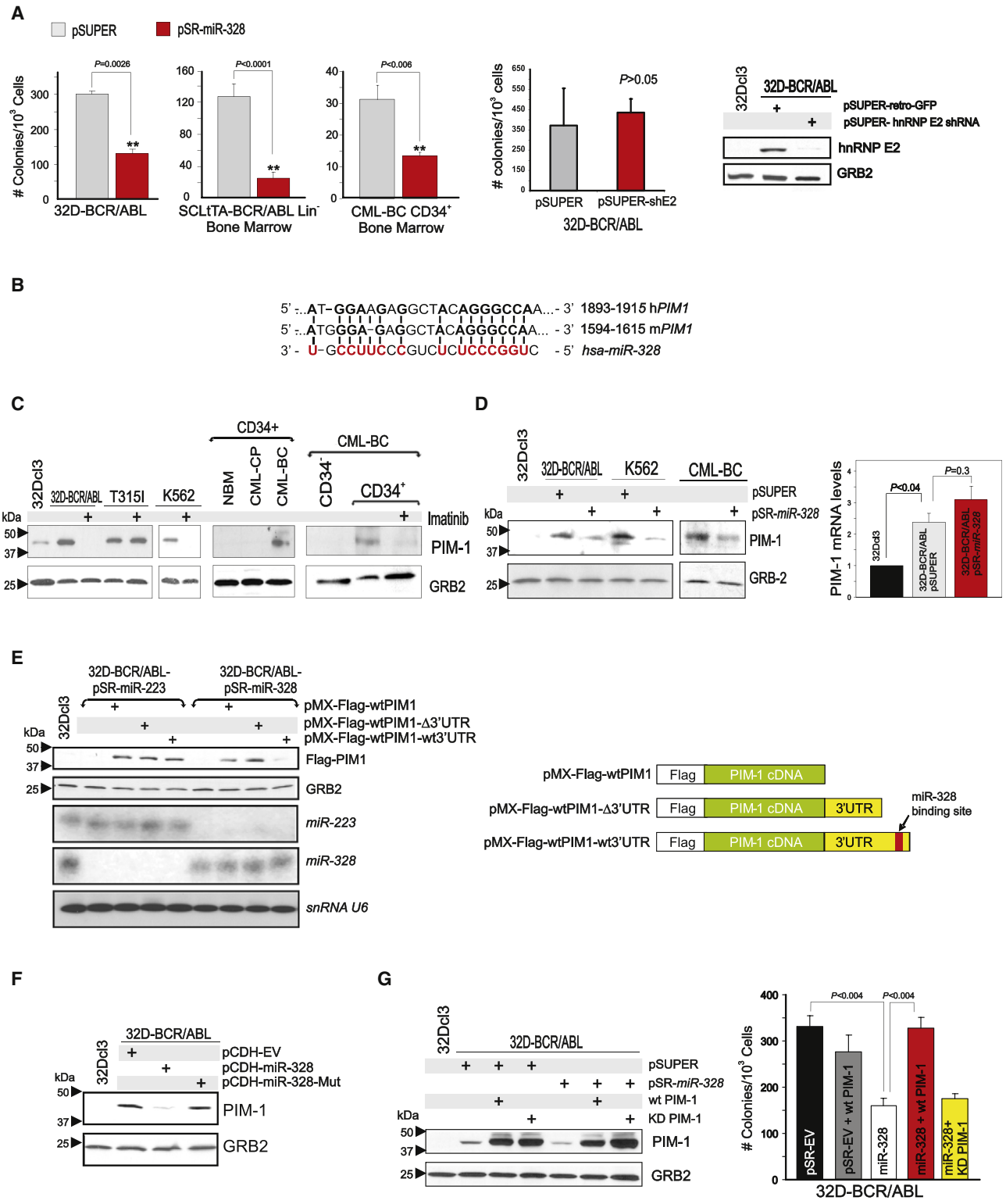

Figure 7. miR-328 Impairs Survival through Targeting of *PIM1* Kinase mRNA

(A) IL-3-independent or -dependent methylcellulose colony formation (mean ± SEM from triplicates of three independent experiments) of vector- (gray bars) and miR-328-transduced (red bars) 32D-BCR/ABL cells (IL-3-independent), leukemic Lin$^-$ SCLtTA-BCR/ABL (n = 5) (IL-3-dependent) cells, CML-BC^{CD34+} (n = 2) (IL-3 dependent) BM progenitors, and vector- (pSUPER) or hnRNP E2 shRNA (pSUPER-shE2)-infected 32D-BCR/ABL cells (IL-3-independent). Inset: Western blot shows hnRNP E2 levels upon shRNA knockdown.

Chendrimada, T.P., Gregory, R.I., Kumaraswamy, E., Norman, J., Cooch, N., Nishikura, K., and Shiekhattar, R. (2005). TRBP recruits the Dicer complex to Ago2 for microRNA processing and gene silencing. Nature *436*, 740–744.

Darnell, J.C., Jensen, K.B., Jin, P., Brown, V., Warren, S.T., and Darnell, R.B. (2001). Fragile X mental retardation protein targets G quartet mRNAs important for neuronal function. Cell *107*, 489–499.

Eiring, A.M., Neviani, P., Santhanam, R., Oaks, J.J., Chang, J.S., Notari, M., Willis, W., Gambacorti-Passerini, C., Volinia, S., Marcucci, G., et al. (2008). Identification of novel posttranscriptional targets of the BCR/ABL oncoprotein by ribonomics: requirement of E2F3 for BCR/ABL leukemogenesis. Blood *111*, 816–828.

Evans, J.R., Mitchell, S.A., Spriggs, K.A., Ostrowski, J., Bomsztyk, K., Ostarek, D., and Willis, A.E. (2003). Members of the poly (rC) binding protein family stimulate the activity of the c-myc internal ribosome entry segment in vitro and in vivo. Oncogene *22*, 8012–8020.

Fazi, F., Rosa, A., Fatica, A., Gelmetti, V., De Marchis, M.L., Nervi, C., and Bozzoni, I. (2005). A minicircuitry comprised of microRNA-223 and transcription factors NFI-A and C/EBPalpha regulates human granulopoiesis. Cell *123*, 819–831.

Ferrari-Amorotti, G., Keeshan, K., Zattoni, M., Guerzoni, C., Iotti, G., Cattelani, S., Donato, N.J., and Calabretta, B. (2006). Leukemogenesis induced by wild-type and STI571-resistant BCR/ABL is potently suppressed by C/EBPalpha. Blood *108*, 1353–1362.

Friedman, R.C., Farh, K.K., Burge, C.B., and Bartel, D.P. (2009). Most mammalian mRNAs are conserved targets of microRNAs. Genome Res. *19*, 92–105.

Fujimura, K., Kano, F., and Murata, M. (2008). Identification of PCBP2, a facilitator of IRES-mediated translation, as a novel constituent of stress granules and processing bodies. RNA *14*, 425–431.

Garzon, R., Fabbri, M., Cimmino, A., Calin, G.A., and Croce, C.M. (2006). MicroRNA expression and function in cancer. Trends Mol. Med. *12*, 580–587.

George, A.D., and Tenenbaum, S.A. (2006). MicroRNA modulation of RNA-binding protein regulatory elements. RNA Biol. *3*, 57–59.

Glisovic, T., Bachorik, J.L., Yong, J., and Dreyfuss, G. (2008). RNA-binding proteins and post-transcriptional gene regulation. FEBS Lett. *582*, 1977–1986.

Guil, S., and Caceres, J.F. (2007). The multifunctional RNA-binding protein hnRNP A1 is required for processing of miR-18a. Nat. Struct. Mol. Biol. *14*, 591–596.

Hinman, M.N., and Lou, H. (2008). Diverse molecular functions of Hu proteins. Cell. Mol. Life Sci. *65*, 3168–3181.

Hoover, R.R., Gerlach, M.J., Koh, E.Y., and Daley, G.Q. (2001). Cooperative and redundant effects of STAT5 and Ras signaling in BCR/ABL transformed hematopoietic cells. Oncogene *20*, 5826–5835.

Jamieson, C.H., Ailles, L.E., Dylla, S.J., Muijtjens, M., Jones, C., Zehnder, J.L., Gotlib, J., Li, K., Manz, M.G., Keating, A., et al. (2004). Granulocyte-macrophage progenitors as candidate leukemic stem cells in blast-crisis CML. N. Engl. J. Med. *351*, 657–667.

Johnnidis, J.B., Harris, M.H., Wheeler, R.T., Stehling-Sun, S., Lam, M.H., Kirak, O., Brummelkamp, T.R., Fleming, M.D., and Camargo, F.D. (2008). Regulation of progenitor cell proliferation and granulocyte function by microRNA-223. Nature *451*, 1125–1129.

Keene, J.D. (2007). RNA regulons: coordination of post-transcriptional events. Nat. Rev. Genet. *8*, 533–543.

Keene, J.D., Komisarow, J.M., and Friedersdorf, M.B. (2006). RIP-Chip: the isolation and identification of mRNAs, microRNAs and protein components of ribonucleoprotein complexes from cell extracts. Nat. Protoc. *1*, 302–307.

Keeshan, K., Santilli, G., Corradini, F., Perrotti, D., and Calabretta, B. (2003). Transcription activation function of C/EBPalpha is required for induction of granulocytic differentiation. Blood *102*, 1267–1275.

Khabar, K.S. (2005). The AU-rich transcriptome: more than interferons and cytokines, and its role in disease. J. Interferon Cytokine Res. *25*, 1–10.

Lal, A., Mazan-Mamczarz, K., Kawai, T., Yang, X., Martindale, J.L., and Gorospe, M. (2004). Concurrent versus individual binding of HuR and AUF1 to common labile target mRNAs. EMBO J. *23*, 3092–3102.

Makeyev, A.V., and Liebhaber, S.A. (2002). The poly(C)-binding proteins: a multiplicity of functions and a search for mechanisms. RNA *8*, 265–278.

Melo, J.V., and Barnes, D.J. (2007). Chronic myeloid leukaemia as a model of disease evolution in human cancer. Nat. Rev. Cancer *7*, 441–453.

Nieborowska-Skorska, M., Hoser, G., Kossev, P., Wasik, M.A., and Skorski, T. (2002). Complementary functions of the antiapoptotic protein A1 and serine/threonine kinase pim-1 in the BCR/ABL-mediated leukemogenesis. Blood *99*, 4531–4539.

Notari, M., Neviani, P., Santhanam, R., Blaser, B.W., Chang, J.S., Galietta, A., Willis, A.E., Roy, D.C., Caligiuri, M.A., Marcucci, G., and Perrotti, D. (2006). A MAPK/HNRPK pathway controls BCR/ABL oncogenic potential by regulating MYC mRNA translation. Blood *107*, 2507–2516.

Ostareck-Lederer, A., and Ostareck, D.H. (2004). Control of mRNA translation and stability in haematopoietic cells: the function of hnRNPs K and E1/E2. Biol. Cell *96*, 407–411.

Parker, R., and Sheth, U. (2007). P bodies and the control of mRNA translation and degradation. Mol. Cell *25*, 635–646.

Perrotti, D., Cesi, V., Trotta, R., Guerzoni, C., Santilli, G., Campbell, K., Iervolino, A., Condorelli, F., Gambacorti-Passerini, C., Caligiuri, M.A., and Calabretta, B. (2002). BCR-ABL suppresses C/EBPalpha expression through inhibitory action of hnRNP E2. Nat. Genet. *30*, 48–58.

Perrotti, D., and Neviani, P. (2007). From mRNA metabolism to cancer therapy: chronic myelogenous leukemia shows the way. Clin. Cancer Res. *13*, 1638–1642.

Rosmarin, A.G., Weil, S.C., Rosner, G.L., Griffin, J.D., Arnaout, M.A., and Tenen, D.G. (1989). Differential expression of CD11b/CD18 (Mo1) and myeloperoxidase genes during myeloid differentiation. Blood *73*, 131–136.

Schultheis, B., Szydlo, R., Mahon, F.X., Apperley, J.F., and Melo, J.V. (2005). Analysis of total phosphotyrosine levels in CD34+ cells from CML patients to predict the response to imatinib mesylate treatment. Blood *105*, 4893–4894.

Tenen, D.G. (2003). Disruption of differentiation in human cancer: AML shows the way. Nat. Rev. Cancer *3*, 89–101.

Vasudevan, S., Tong, Y., and Steitz, J.A. (2007). Switching from repression to activation: microRNAs can up-regulate translation. Science *318*, 1931–1934.

Venturini, L., Battmer, K., Castoldi, M., Schultheis, B., Hochhaus, A., Muckenthaler, M.U., Ganser, A., Eder, M., and Scherr, M. (2007). Expression of the miR-17-92 polycistron in chronic myeloid leukemia (CML) CD34+ cells. Blood *109*, 4399–4405.

Wagner, K., Zhang, P., Rosenbauer, F., Drescher, B., Kobayashi, S., Radomska, H.S., Kutok, J.L., Gilliland, D.G., Krauter, J., and Tenen, D.G. (2006). Absence of the transcription factor CCAAT enhancer binding protein alpha results in loss of myeloid identity in bcr/abl-induced malignancy. Proc. Natl. Acad. Sci. USA *103*, 6338–6343.

Wang, C.H., Lee, D.Y., Deng, Z., Jeyapalan, Z., Lee, S.C., Kahai, S., Lu, W.Y., Zhang, Y., and Yang, B.B. (2008). MicroRNA miR-328 regulates zonation morphogenesis by targeting CD44 expression. PLoS ONE *3*, e2420.

Wang, W., Wang, X., Ward, A.C., Touw, I.P., and Friedman, A.D. (2001). C/EBPalpha and G-CSF receptor signals cooperate to induce the myeloperoxidase and neutrophil elastase genes. Leukemia *15*, 779–786.

Zalfa, F., Giorgi, M., Primerano, B., Moro, A., Di Penta, A., Reis, S., Oostra, B., and Bagni, C. (2003). The fragile X syndrome protein FMRP associates with BC1 RNA and regulates the translation of specific mRNAs at synapses. Cell *112*, 317–327.

EXTENDED EXPERIMENTAL PROCEDURES

Cell Cultures and Primary Cells

32Dcl3 murine myeloid precursor cells, Ph1(+) erythroleukemia K562 cells, and derivative lines were maintained in IMDM plus 10% FBS and 2 mM L-glutamine (GIBCO). 10% WEHI-conditioned medium was used as the source of mIL-3. 293T cells were maintained in culture in DMEM, 10% FBS and 2 mM L-glutamine. 32D-BCR/ABL, 32D-BCR/ABL(T315I), and miRNA-expressing cells were generated by retroviral infection followed by antibiotics-mediated selection or FACS-mediated sorting of GFP^+ cells (Perrotti et al., 2002). Newly established 32D-BCR/ABL cells (which express *CEBPA* mRNA but not C/EBPα protein) (Perrotti et al., 2002) were used in differentiation assays. Murine BM cells from femurs of C57BL/6 or leukemic SCLtTA-BCR/ABL mice (Koschmieder et al., 2005) underwent Lin^- magnetic-activated cell sorting (MACS, Miltenyi Biotech) and were grown for 2 days in IMDM medium containing murine IL-3 (2 ng/ml), IL-6 (2 ng/ml), SCF (10 ng/ml), Flt3-ligand (5 ng/ml), and GM-CSF (5 ng/ml) (R&D Systems) prior to infection with MigR1, MigR1-$p210^{BCR/ABL}$ (W. Pear, UPENN, Philadelphia, PA), or miRNA retroviral vectors. All animal studies were performed with approval of The OSU Institutional Animal Care and Use Committee. For patient specimens, frozen mononuclear BM cells of unidentified CML-CP (91%–100% Ph1(+) by FISH) and myeloid CML-BC patients were Ficoll separated, cultured o/n in IMDM plus 30% FBS, 2mM L-glutamine supplemented with IL-3 (20 ng/ml), IL-6 (20 ng/ml), Flt-3 ligand (100 ng/ml), and KL (100 ng/ml) (Stem Cell Technologies), and the $CD34^+$ fraction was isolated using the CD34 MultiSort kit (Miltenyi Biotec). Frozen samples of $CD34^+$ BM cells from healthy donors were purchased from Cincinnati Children's Hospital, Cincinnati, OH. Patient specimens were obtained from the OSU Leukemia Tissue Bank, Columbus OH; Maisonneuve-Rosemont Hospital, Montreal, Quebec, Canada; City of Hope National Medical Center, Duarte, CA; MD Anderson Cancer Center, Houston TX; and Aarhus University, Denmark. All the performed experiments were approved by The OSU Institutional Review Board. Where indicated, cells were treated with the following kinase inhibitors: 1–2 μM imatinib mesylate (Novartis Oncology), 25 μM U0126 (Promega), or 10 μM CI-1040 (Pfizer).

In Vitro and In Vivo Differentiation Assays

In vitro granulocytic differentiation was induced by exposing cells to 25 ng/ml rhG-CSF for 7–10 days. Morphologic differentiation was assessed by Wright/Giemsa staining of cytospins. miR-328 expression in different lineages was extrapolated from miRNA array analysis of hematopoietic precursors obtained by culturing for 14 days human (non-mobilized) $CD34^+$ BM cells (n = 2) in EPO/SCF/IL-3 (erythroid), G-CSF/GM-CSF/SCF/IL-6/IL-3 (granulocytic), TPO/SCF/IL-3 (megakaryocytic) and M-CSF/GM-CSF/IL-6/IL-3/SCF (monocytic). Morphology and lineage-specific antibody staining was used to assess differentiation. Total RNA from lineage-committed cells at different days of culture was hybridized in duplicate to OSU v3.0 miRNA chip. After quantiles normalization, differentially expressed miRNAs were identified by using the univariate t test within the BRB array tools. For in vivo differentiation, 10-week-old ICR-SCID mice (n = 13 per group) were i.v. injected (5×10^5 cells/mouse) with pSUPERIOR.retro.puro- or pSUP-miR-328-transduced 6.15-WT-uORF-CEBPA(GFP^+) cells. Engraftment was assessed 1 week after cell injection by nested RT-PCR-mediated detection of BCR/ABL transcripts in circulating peripheral blood cells (Eiring et al., 2008). After 3 weeks, mice were sacrificed and BM, spleen, and liver were subjected to visual and histological (H&E staining) analyses and flow-cytometric detection of $Gr1^+GFP^+$ BM cells using PE-conjugated GR1 mAb (PharMingen). Light microscopy was performed on a Zeiss Axioskop 2 Plus microscope equipped with a Plan-Neo 40×/0.75NA objective and a Canon Powershot A70 camera. Images were captured using Canon Remote Capture software and Adobe Photoshop CS.

Plasmids

The pSRαMSVtkneo-BCR/ABL, pMSCVpuro-Flag-hnRNP E2, MigRI-HA-CEBPA, pcDNA3-WTuORF-C/EBPα constructs have been described (Perrotti et al., 2002).

pSUPER-shE2

The human hnRNP E2 sequence targeting human and mouse mRNAs was subcloned into the pSUPER.retro.neo.GFP vector as previously described (Eiring et al., 2008).

pSR- and pCDH-miR-223, pSR- and pCDH-miR-328, pCDH-miR-328-Mut, pSUP-miR-328, and pSUP-miR-181b

Pre-miR-328, pre-miR-223, and pre-miR-181b were PCR amplified from 32Dcl3 genomic DNA (see below for primer sequences) and cloned into either the retroviral pSuper.retro.neo.GFP or pSuperior.retro.puro vectors (OligoEngine), or the lentiviral pCDH-CMV-MCS-EF1-copGFP vector (System Biosciences). The p*CDH-miR-328-Mut* vector was mutated in the seed sequence with the QuikChange Site-Directed Mutagenesis kit (Stratagene) according to the manufacturer's instructions.

pMX-Flag-WTPIM1-WT3′UTR and pMX-Flag-WTPIM1-Δ3′UTR (Deleted of the miR-328-Binding Site)

The wild-type (658 base pairs) or 3′-deleted (462 base pairs) *PIM1* 3′UTRs were RT-PCR amplified from 32D-BCR/ABL mRNA (see below for primer sequences) and cloned into the pMX-Flag-WTPIM1 plasmid. pMX-Flag-WTPIM1 and pMX-Flag-KD-PIM1 have been described (Nieborowska-Skorska et al., 2002).

Cloning Primers and Sequences

pSUPER.retro.neo.GFP

miR-223 Forward: 5′-CATAGATCTTCCAGTTGCACATCTTCCAGC-3′
miR-223 Reverse: 5′-CATAAGCTTAAAAAGAGAGCTTCATGTTTCATAAGC-3′
miR-328 Forward: 5′-CATAGATCTAAGAGCTCATGGAAACTGTGG-3′
miR-328 Reverse: 5′-CATAAGCTTAAAAAACAGCGTTGCTGTGTGAGCT-3′

pSUPERIOR.retro.puro

miR-328 Forward: 5′-CATAGATCTAAGAGCTCATGGAAACTGTGG-3′
miR-328 Reverse: 5′-CATAAGCTTAAAAAACAGCGTTGCTGTGTGAGCT-3′
miR-181b Forward: 5′-CATAGATCTGGCTGGTTACTAAGGGAGAA-3′
miR-181b Reverse: 5′-CATAAGCTTAAAAAGTAGCAGCTCCCACTCACA-3′

pCDH-CMV-MCS-EF1-copGFP

miR-223 Forward: 5′-CATGAATTCTCCAGTTGCACATCTTCCAGC-3′
miR-223 Reverse: 5′-CATGGATCCAAAAAAGAGAGCTTCATGTTTCATAAGC-3′
miR-328 Forward: 5′-CATGAATTCAAGAGCTCATGGAAACTGTGG-3′
miR-328 Reverse: 5′-CATGGATCCAAAAAAACAGCGTTGCTGTGTGAGCT-3′
miR-328-Mut Primer #1: 5′-GAAAGTATCTACAGCCCCATTCCCGCTCTGCCCTTCCGTCC-3′
miR-328-Mut Primer #2: 5′-GGACGGAAGGGCAGAGCGGGAATGGGGCTGTAGATACTTTC-3′

pMX-Flag-WTPIM1

WT3′UTR Forward: 5′-CATGCGGCCGCCAGCCTTTCTGCTGCTGTC-3′
WT3′UTR Reverse: 5′-CATGCGGCCGCTTGTGCGTTCTGTGTGAGGT-3′
Δ3′UTR Forward: 5′-CATGCGGCCGCCAGCCTTTCTGCTGCTGTC-3′
Δ3′UTR Reverse: 5′-CATGCGGCCGCCCAGGCAGAGTTTGAGAAGC-3′

RNA Extraction, Northern Blot, and Real-Time PCR

Total RNA was used in northern blot, RT-PCR, and/or qRT-PCR for the analysis of miRNA and mRNA expression levels. qRT-PCR for detection of *CEBPA* mRNA levels was performed using the PCR primers indicated below. Total RNA was isolated using Trizol (Invitrogen) and analyzed for miRNA expression by northern blot and/or qRT-PCR. For northern blot, RNA (1–20 μg) was fractionated on a 15% denaturing polyacrylamide-urea gel (Bio-Rad) and subject to hybridization (18 hr; 43°C) with ^{32}P-labeled miR-223, miR-328, miR-328-Mut, or U6 snRNA probes (see below for probe sequences).

Northern Hybridization Probes and Sequences

miR-328: 5′-ACGGAAGGGCAGAGAGGGCCAG-3′
miR-328-Mut: 5′-GGACGGAAGGGCAGAGCGGGAATG-3′
snRNA U6: 5′-GCAGGGGCCATGCTAATCTTCTCTGTATCG-3′
miR-223: 5′-GGGGTATTTGACAAACTGACA-3′

For qRT-PCR, mature miR-328, miR-223, and miR-181b, as well as U6 snRNA looped primers were used according to the manufacturer's instructions (Applied Biosystems). Where indicated, resulting PCR products were fractionated on a 15% denaturing polyacrylamide-urea gel (Bio-Rad) and subject to staining with ethidium bromide. qRT-PCR for detection of *PIM1* and *SET* mRNA levels was performed as described (Harb et al., 2008; Neviani et al., 2005). qRT-PCR for detection of *CEBPA* mRNA levels was performed using the PCR primers indicated below. U6 snRNA and GAPDH levels were analyzed for normalization of miRNA and mRNA PCRs, respectively.

REMSA, UV Crosslinking, and RNA Immunoprecipitation

Recombinant MBP-hnRNP E2 (Chang et al., 2007) and 32Dcl3 or 32D-BCR/ABL cytoplasmic extracts were used in REMSA and UV crosslinking as described (Perrotti et al., 2002). Briefly, reactions performed with 1 μg MBP-hnRNP E2 or 10 μg cytoplasmic extracts were incubated (30 min, RT) with a ^{32}P-labeled miR-328, miR-328-Mut, miR-330, miR-181b, or *CEBPA* uORF (Perrotti et al., 2002) oligoribonucleotide and resolved in 5% native-PAGE/0.5X TBE for REMSA or in 4%–15% SDS-PAGE for UV crosslinking analysis (see below for RNA oligonucleotide probe sequences). For competition assays, 500- to 2000-fold molar excess of single-stranded oligoribonucleotides was added to the reaction. RNA immunoprecipitation (RIP) was performed as described (Keene et al., 2006). Briefly, 32D-BCR/ABL, 32D-Flag-E2, 32D-BCR/ABL-Flag-E2, and 6.15-WTuORF cells were transduced with either pSR-miR-328, pSUP-miR-328, pSUP-miR-181b, or the empty vector, lysed (5 min, 0°C) in 100 mM KCl, 5 mM $MgCl_2$, 10 mM HEPES [pH 7.0], 0.5% NP40, 1 mM DTT, 100 units/ml RNase OUT (Invitrogen), 400 μM vanadyl-ribonucleoside complex and protease inhibitors (Roche), clarified and stored o/n at −80°C. Ribonucleoprotein particle-enriched lysates were incubated with either protein G- (anti-Flag or anti-HA), sepharose A- (anti-Dicer, anti-hnRNP E2, and rIgG), or sepharose A/agarose G-coupled beads (anti-Ago2 and rIgG) (4°C; 2 h). Beads were subsequently washed four times with 50 mM TRIS/HCl, pH 7.0, 150 mM NaCl, 1 mM $MgCl_2$, and 0.05% NP-40, and twice after addition of 1M Urea. IPs were digested with proteinase K (55°C; 30′) and hnRNP E2-associated mRNAs

and miRNAs were isolated as described above. RT-PCR for *CEBPA* was performed with the PCR primers indicated below. RT-PCR for miR-328 was performed as described (Wang et al., 2008).

RNA Oligonucleotides and Sequences

miR-328: 5′-CUGGCCCUCUCUGCCCUUCCGU-3′
miR-328-Mut: 5′-CAUUCCCGCUCUGCCCUUCCGU-3′
miR-330: 5′-GCAAAGCACACGGCCUGCAGAGA-3′
miR-181b: 5′-AACAUUCAUUGCUGUCGGUGGGU-3′
CEBPA uORF: 5′-CUGGCCAUGCCGGGAGAACUCUAACUCCCCCAUGGAG-3′

Western Blotting and Coimmunoprecipitation

For Western blot, 1×10^7 cells were lysed (0°C; 30 min) in 50–100 μl RIPA buffer (150 mM NaCl, 1% NP40, 0.1% SDS, 50 mM Tris [pH 8.0]) containing 1 mM PMSF, 25 μg/ml aprotinin, 10 μg/ml leupeptin, 100 μg/ml pepstatin A, 5 mM benzamidine, 1 mM Na_3VO_4, 50 mM NaF, 10 mM β-glycerol-phosphate, clarified (12,000 × g; 4°C, 30′), and subjected to SDS-PAGE. For C/EBPα detection, 10^6 cells were directly lysed in 20 μl Laemmli buffer and denatured prior to SDS-PAGE and transfer to nitrocellulose. For coimmunoprecipitation, cells were lysed on ice with immunoprecipitation buffer (10 mM HEPES, pH 7.4, 150 mM NaCl, 1% NP-40, and 0.1% SDS) supplemented with protease (Complete EDTA free, Roche) and phosphatase (PhosStop, Roche) inhibitors. 1.0 mg of protein in 200 μl of buffer was incubated with 25 μl of sepharose A beads previously coated with 4 μg of antibody (2 hr, 4°C). Half of the immunoprecipitate was then separated by SDS-PAGE and transferred to nitrocellulose. Antibodies used were: rabbit polyclonal anti-hnRNP E2 (Chkheidze et al., 1999; Gamarnik and Andino, 1997; Waggoner and Liebhaber, 2003); anti-PIM1, anti-C/EBPα, anti-NFI-A, anti-Dicer, clone H-212, and anti-TRBP2, clone S-11 (Santa Cruz Biotechnology); anti-phosphotyrosine, clone 4G10 (Upstate); anti-GRB2 (BD Transduction Laboratories); anti-HA.11 (Covance); anti-Flag, clone M2 (Sigma); and anti-Ago2, clone C34C6 (Cell Signaling). Rabbit IgG (rIgG) antibody (Santa Cruz Biotechnology, Inc.) served as an isotype control.

Chromatin Immunoprecipitation

ChIP assays were performed using an EZ-Chip kit (Millipore). Briefly, MigR1-HA-C/EBPα-transduced (Perrotti et al., 2002) 32Dcl3 cells were formaldehyde-crosslinked, lysed and incubated with protein G-coupled anti-HA.11 and anti-Flag (negative control) antibodies for immunoprecipitation (IP) of ectopic HA-C/EBPα. C/EBPα-bound DNA was PCR amplified with primers for the four putative C/EBPα-binding sites located upstream of the mouse *pre-miR-328* gene (see below for PCR primer sequences).

PCR Primers and Sequences

C/EBPα ChIP: *miR-328* Primers
CEBP1 Forward: 5′-CCACAGGTAGAACTAAGGATGGAC-3′
CEBP1 Reverse: 5′-CTTTCTCCATCAGCTATGACCAC-3′
CEBP2 Forward: 5′-AGGTATGTGGCCTATAGGGAGAG-3′
CEBP2 Reverse, 5′-AAGCTATGGTTTTGCTGTTTATCC-3′
CEBP3 Forward: 5′-GAGTGATGAGAGGGCTCTGG-3′
CEBP3 Reverse: 5′-CTGGTTAACGACTCTCAATCGTC-3′
CEBP4 Forward: 5′-ATAGGTGAGGGCATTCACTTTG-3′
CEBP4 Reverse: 5′-CTGAATAAGACCTGGAAGGAGATG-3′
***CEBPA* RT-PCR Primers**
CEBPA Forward: 5′-GCGAGCACGAGACGTCTATAGA-3′
CEBPA Reverse: 5′-GCCAGGAACTCGTCGTTGAA-3′

SUPPLEMENTAL REFERENCES

Chkheidze, A.N., Lyakhov, D.L., Makeyev, A.V., Morales, J., Kong, J., and Liebhaber, S.A. (1999). Assembly of the alpha-globin mRNA stability complex reflects binary interaction between the pyrimidine-rich 3′ untranslated region determinant and poly(C) binding protein alphaCP. Mol. Cell. Biol. *19*, 4572–4581.

Gamarnik, A.V., and Andino, R. (1997). Two functional complexes formed by KH domain containing proteins with the 5′ noncoding region of poliovirus RNA. RNA *3*, 882–892.

Harb, J.G., Chyla, B.I., and Huettner, C.S. (2008). Loss of Bcl-x in Ph+ B-ALL increases cellular proliferation and does not inhibit leukemogenesis. Blood *111*, 3760–3769.

Koschmieder, S., Gottgens, B., Zhang, P., Iwasaki-Arai, J., Akashi, K., Kutok, J.L., Dayaram, T., Geary, K., Green, A.R., Tenen, D.G., and Huettner, C.S. (2005). Inducible chronic phase of myeloid leukemia with expansion of hematopoietic stem cells in a transgenic model of BCR-ABL leukemogenesis. Blood *105*, 324–334.

Neviani, P., Santhanam, R., Trotta, R., Notari, M., Blaser, B.W., Liu, S., Mao, H., Chang, J.S., Galietta, A., Uttam, A., et al. (2005). The tumor suppressor PP2A is functionally inactivated in blast crisis CML through the inhibitory activity of the BCR/ABL-regulated SET protein. Cancer Cell *8*, 355–368.

Waggoner, S.A., and Liebhaber, S.A. (2003). Identification of mRNAs associated with alphaCP2-containing RNP complexes. Mol. Cell. Biol. *23*, 7055–7067.

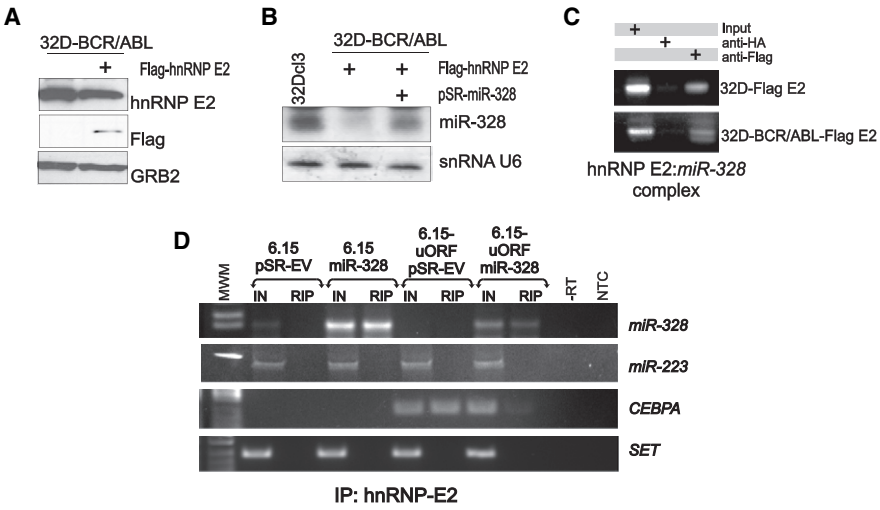

Figure S1. miR-328 Competes with *CEBPA* mRNA for Binding to hnRNP E2, Related to Figure 2

(A) Western blot shows levels of Flag-tagged and endogenous hnRNP E2 in parental and Flag-hnRNP E2-expressing 32D-BCR/ABL cells. GRB2 levels were analyzed for controls.

(B) Northern blot shows levels of miR-328 in 32Dcl3 (lane 1), in vector- (lane 2) and in pSR-miR328-transduced (lane 3) 32D-BCR/ABL-Flag-E2 cells. snRNA U6 levels served as a loading control.

(C) RIP assay shows association of mature miR-328 to ectopic hnRNP E2 in anti-Flag RIPs from miR-328-expressing 32D-Flag-E2 and 32D-BCR/ABL-Flag-E2 cells. Anti-HA RIPs were used as negative controls.

(D) RIP assay shows association of miR-328 and *CEBPA* mRNA, but not miR-223 or *SET* mRNA, to endogenous hnRNP E2 in anti-hnRNP E2 RIPs from empty vector- and miR-328-expressing 6.15 and 6.15-uORF cells.

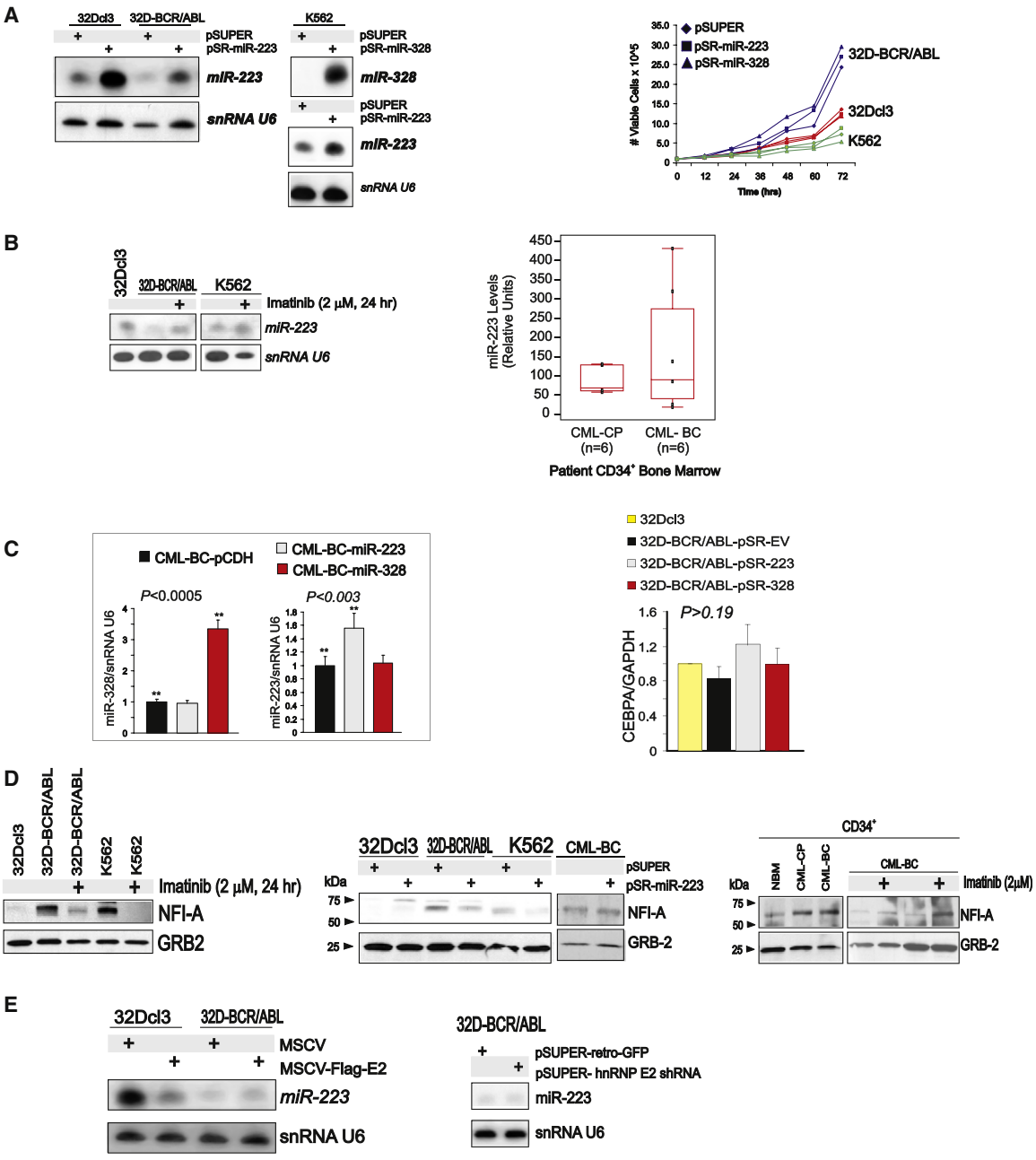

Figure S2. Regulation of miR-223 Expression in BCR/ABL$^+$ Cells, Related to Figure 4

(A) Levels of ectopic miR-223 or miR-328 (left) and their effect on proliferation of (right) 32Dcl3, 32D-BCR/ABL, and K562 cells.

(B) Left: Northern blot and qRT-PCR analyses show expression of miR-223 in 32Dcl3, untreated and imatinib-treated BCR/ABL$^+$ cell lines. Right: qRT-PCR analyses show expression of miR-223 in CD34$^+$ bone marrow progenitors from CML-CP (n = 6) and CML-BC (n = 6) patients (mean ± SEM). U6 snRNA was used for normalization. Notably, qRT-PCR revealed no significant changes (p = 0.35) in miR-223 levels in CML-BC^{CD34+} (n = 6) versus CML-CP^{CD34+} (n = 6) BM cells (mean ± SEM).

(C) Left: qRT-PCR shows levels of miR-223 and miR-328 in vector (pCDH)-, miR-223-, and miR-328-infected CML-BC progenitors (mean ± SEM). Right: qRT-PCR shows levels of *CEBPA* in empty vector-, miR-223-, or miR-328-infected 32D-BCR/ABL cells (mean ± SEM).

(D) Left: Western blot shows that NFI-A expression is induced in a BCR/ABL kinase-dependent manner. Middle: Ectopic miR-223 could efficiently reduce NFI-A levels in 32D-BCR/ABL and K562 cells. Right: By contrast, NFI-A was not influenced by ectopic miR-223 expression in CML-BC^{CD34+} progenitors. While NFI-A was slightly induced in CML-CP^{CD34+} compared to CD34$^+$ progenitors from normal bone marrow (NBM^{CD34+}), its expression was not different in CML-CP^{CD34+} versus CML-BC^{CD34+} progenitors (n = 2), and was inhibited rather than induced by imatinib treatment (n = 3).

(E) Left: Northern blot analysis shows miR-223 levels in parental and Flag-hnRNP E2-expressing 32Dcl3 and 32D-BCR/ABL cells. Right: Effect of shRNA-mediated hnRNP E2 downregulation on miR-223 levels. U6 snRNA and GRB2 protein levels were used as controls.